THE SURFACE ABUNDANCE OF TITANIUM ON MERCURY. L. R. Nittler[1,*], C. Cartier[2], B. Charlier[3], E. Crapster-Pregont[4], E. A. Frank[1,5], O. Namur[6], R. D. Starr[7,8], A.Vorburger[2,9], S. Z. Weider[1], [1]Department of Terrestrial Magnetism, Carnegie Institution of Washington, Washington, DC 20015, USA, [2]Laboratoire Magmas et Volcans, Université Blaise Pascal, Clermont-Ferrand 63038, France, [3]Département de Géologie, Université de Liège, 4000 Sart Tilman, Belgium, [4]Department of Earth and Planetary Sciences, American Museum of Natural History, New York, NY 10024, USA, [5]First Mode, 500 Yale Ave N, Seattle, WA 98109, USA, [6]Department of Earth and Environmental Sciences, KU Leuven, Leuven, 3001, Belgium [7]Physics Department, The Catholic University of America, Washington, DC 20064, USA, [8]Solar System Exploration Division, NASA Goddard Space Flight Center, Greenbelt, MD 20771, USA, [9]Physics Institute, University of Bern, Bern, Switzerland. *E-mail: lnittler@ciw.edu

Introduction: The X-Ray Spectrometer (XRS) and Gamma-Ray and Neutron Spectrometer (GRNS) on the MErcury Surface, Space ENvironment, GEochemistry, and Ranging (MESSENGER) spacecraft were used to map Mercury's surface composition in a number of geochemically important elements during MESSENGER's four-year orbital mission [1-4]. The geochemical measurements revealed Mercury's crust to be surprisingly rich in volatile elements, including S, Na, K, Cl, and C, and to be enriched in Mg and depleted in Al, Ca, and Fe, relative to other terrestrial planets.

The XRS detected fluorescent emissions, induced by X-rays emitted from the Sun's corona, from the top tens of micrometers of the planetary regolith. During large solar flares, the coronal X-ray flux increased by orders of magnitude, enabling detection of heavier and/or less abundant elements, including S, Ca, Ti, Cr, and Fe. We recently reported a reanalysis of the full-mission XRS solar flare data set to derive a map of Cr abundances across Mercury, as this element may potentially be a useful oxybarometer [5]. Here we focus on deriving the best possible estimate of the surface Ti abundance and its uncertainty from the XRS dataset, as this element has potential to constrain the thickness of a putative FeS layer at the base of Mercury's mantle [6]. Because of the need for large flares to detect Ti and its low abundance (<1 wt%), Ti data have been previously reported for only 25 flares [1, 7]; we extend the analysis here to a total of 233 XRS measurements across the planet's surface.

Methods: The relatively poor energy resolution of the XRS gas-proportional counter detectors results in Ti appearing in XRS spectra only as a high-energy shoulder on the Ca peak (see Figure S6 of [1]), but this shoulder can be well-fitted by the least-squares methodology used to extract abundances from XRS data [1], provided the signal is high enough. More than 2000 individual flare XRS spectra acquired from throughout the entire 2011-2015 MESSENGER orbital mission were previously fit to extract elemental abundances and generate chemical maps of Mercury's surface [2, 8]. Of these analyses, 672 had non-zero Ti detections. We used a number of criteria to identify the most reliable Ti measurements from this data set: i) we excluded data acquired from flares with inferred solar coronal plasma temperatures below 15 MK as there was very large scatter in measured Ti/Si ratios for lower flare temperatures; ii) flares found to have unusually high detector backgrounds at high energy were excluded, since such backgrounds could significantly affect results for low-abundance elements like Ti; iii) the major-element (Mg/Si, Al/Si, S/Si, and Ca/Si) results for each remaining flare analysis were compared with those in the global maps of these elements for the same area of the surface. Results that strongly diverged from the global maps, which are based on multiple overlapping measurements and hence are considered to be more accurate than individual analyses, for one or more element ratio were excluded; and iv) a few measurements were excluded because they had derived Ti/Si ratios much higher than other measurements with overlapping footprints.

Results and Discussion: The measured Ti/Si ratios are plotted against Mg/Si and Al/Si ratios for the 233 remaining flare analyses in Figure 1. The Mg/Si and Al/Si ratios for these points are taken from the global maps [2, 8] for the XRS footprints corresponding to the Ti measurements.

The average Ti/Si ratio for the entire data set is 0.0083 with a standard deviation of 0.0040; excluding the 57 analyses which lie within 2σ of zero gives 0.0098 ±0.0030. Ti and Al are not expected to fractionate from one another during the early stages of igneous differentiation, so a correlation might be expected between Ti/Si and Al/Si. The large errors in Ti/Si ratios, as well as a rather limited range of Mg/Si and Al/Si ratios for most of the points for which we have Ti data (Fig. 1), make it difficult to resolve such a correlation in the data. Nonetheless, a constant Ti/Al ratio is supported by the fact that the three measurements from within the so-called high-Mg region [8, 9], which also has the lowest Al/Si ratios on the planet, all have low Ti/Si ratios (dashed ellipses in Fig. 1).

Accurate estimates of the average Mercury Ti/Al ratio and its error are needed to constrain the nature of any FeS layer within Mercury [6]. Unfortunately, the calculated average depends strongly on which data are included in average, and the overall low Ti abundance

and relatively large errors bars for many data points may lead to biases. The spread in the data reflects both statistical errors and any additional systematic uncertainty introduced by the XRS technique.

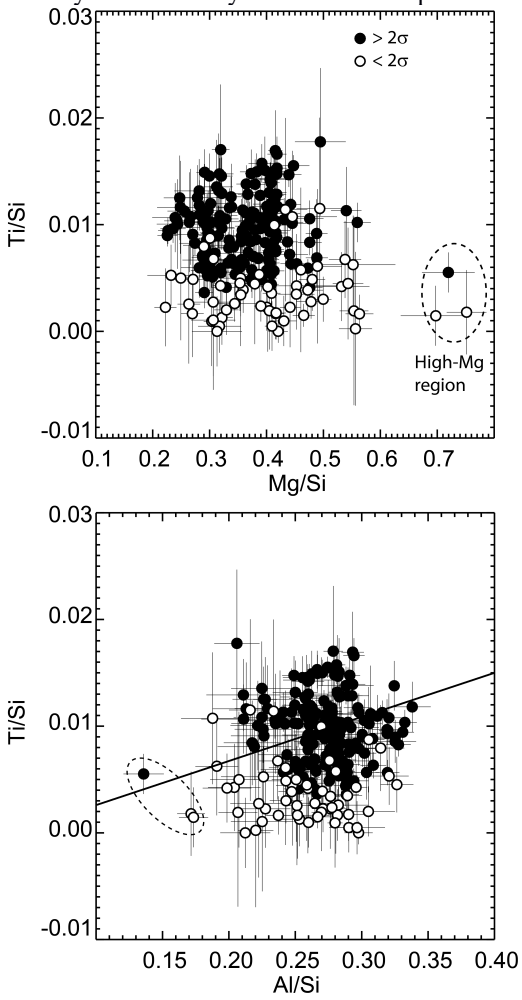

Figure 1. Ti/Si, Mg/Si, and Al/Si ratios derived from 233 MESSENGER XRS flare observations.

To better estimate the average Ti/Al ratio and its error, we took a Monte Carlo approach and generated simulated data to compare with the observations. Each simulated "measurement" was drawn randomly from a population with a single average Ti/Al ratio (*r)* and an assumed intrinsic systematic uncertainty for the XRS method (σ_{syst}), representing the limiting uncertainty with which we can determine the average Ti/Al ratio, and assigned a statistical uncertainty taken randomly from the actual XRS flare measurements. Once a simulated dataset of 233 points was generated for given values of *r* and σ_{syst}, the average and standard deviation of the resulting Ti/Al distribution was calculated and compared to the observed data. In both simulated and observed datasets, only data that differ from zero by more than two sigma were included. This process was repeated 100 times each for a range of values of *r* and σ_{syst}. The best match to the observed data was found for $r = 0.0345$ and $\sigma_{syst} = 0.008$ (Fig. 2); we take these values to be the best estimate of the average Ti/Al ratio of Mercury's surface and its uncertainty. The solid line in Fig. 1 (bottom) indicates the correlation line between Ti/Si and Al/Si corresponding to this value of Ti/Al. Our best derived Ti/Al value of 0.0345 is consistent with there being a thin or no FeS layer in Mercury [6]. It is also lower than that of enstatite chondrites (Ti/Al=0.05), thought to be analogs of Mercury's starting materials, perhaps suggesting some extraction of Ti into the planet's metallic core.

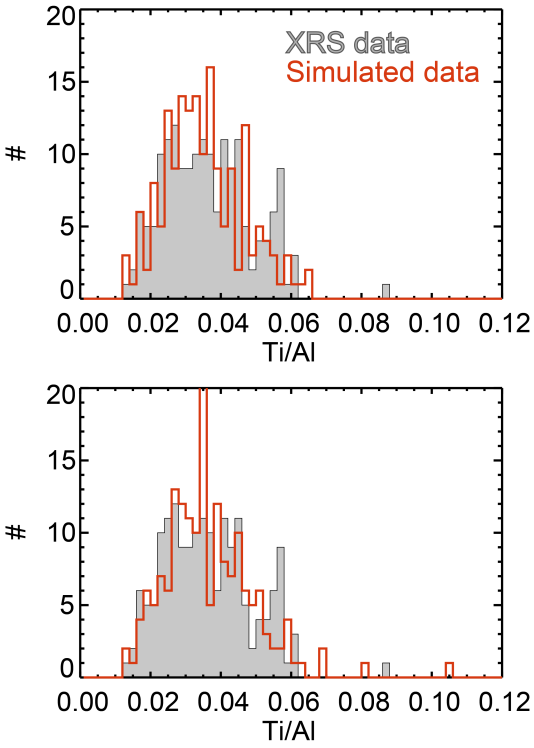

Figure 2. Two simulated Ti/Al distributions compared to observed Mercury data set for best-fit Monte Carlo parameters: $r = 0.0345$ and $\sigma_{syst} = 0.008$.

References: [1] Nittler L. R., et al. (2011) *Science, 333,* 1847–1850. [2] Nittler L. R., et al., (2018) in *Mercury: The View after MESSENGER*, Cambridge Univ. Press, pp. 30–51. [3] Peplowski P. N., et al. (2011) *Science, 333,* 1850–1852. [4] Evans L. G., et al. (2012) *JGR: Plan., 117,* E00L07. [5] Nittler L. R., et al. (2018) *LPS 49,* Abstract #2070. [6] Cartier C., et al. (2017) *LPS 48,* Abstract #1419. [7] Weider S. Z., et al. (2014) *Icarus, 235,* 170–186. [8] Weider S. Z., et al. (2015) *EPSL, 416,* 109–120. [9] Frank E. A., et al. (2017) *JGR: Plan., 122,* 614–632.